1000

Milek

ANALYTICAL STUDY OF PANEL ZONE BEHAVIOR IN BEAM-COLUMN CONNECTIONS

for

THE AMERICAN INSTITUTE
of
STEEL CONSTRUCTION, INC.

by

Ralph M. Richard

and

David R. Pettijohn

November 1981

Department of Civil Engineering
and Engineering Mechanics

The University of Arizona
Tucson, Arizona

ANALYTICAL STUDY OF PANEL ZONE BEHAVIOR IN BEAM-COLUMN CONNECTIONS

for

THE AMERICAN INSTITUTE
of
STEEL CONSTRUCTION, INC.

by

Ralph M. Richard

and

David R. Pettijohn

November 1981

Department of Civil Engineering
and Engineering Mechanics

The University of Arizona
Tucson, Arizona

ANALYTICAL STUDY OF PANEL ZONE BEHAVIOR
IN BEAM COLUMN CONNECTIONS

I. Introduction.

The panel zones of a series of four test specimens comprising a W14 x 90 column section and a W24 x 62 beam section were analyzed using the nonlinear finite element program INELAS. The results of these analyses are compared with those obtained experimentally by Dr. Roger G. Slutter of the Fritz Engineering Laboratory at Lehigh University (1). The test specimen configurations and designs are shown in Figure 1.

II. Program INELAS.

Program INELAS (2) is a finite element program written to analyze structural systems stressed into the inelastic range. This program was written by Professor Ralph M. Richard of the University and has been used extensively in the aerospace industry since the late 1960's and more recently in the civil engineering profession in research studies for the analysis and design of steel connections. Included in the program are the following elements:

1) A constant strain bar.
2) A constant strain plane triangle.
3) An orthotropic constant strain plane triangle.
4) A linear strain plane rectangle.
5) A plane linear strain quadrilateral.
6) A connector element to represent bolts, rivets or weldments.

Mixed boundary conditions may be treated; i.e., either forces or prescribed displacements may be specified. Three-dimensional structures consisting of two-dimensional (i.e., plane) elements may be modeled.

The nonlinear structural response for the two-dimensional elements is calculated by a numerical algorithm that uses the von Mises yield criterion and the associated flow rule (3). Ordinary simultaneous first-order differential equations are generated to describe differential force-displacement relationships and are solved by the fourth-order Runge Kutta method.

III. The Finite Element Models.

The general finite model of the test specimens and loading is shown in Figure 2. Specimen No. 1 (no doubler plate) consisted of 54 plane stress finite elements (rectangles, quadrilaterals, and triangles) which simulated the beam and column webs and 46 bar elements which simulate the beam and column flanges and the beam flange continuity plates. A comparison of the deflection at the applied load points as shown in Figure 1 obtained by beam theory with the deflection obtained by the finite element model indicates that the model predicts the elastic structural behavior of the test specimen within two percent.

Specimens 2, 3, and 4 were modeled the same as Specimen 1 except linear strain rectangular plate elements were added to simulate the doublers and weldment elements were used to attach these plates to the column web as shown in Figure 2.

Material uniaxial stress-strain properties used to represent the A36 and Grade 50 steels are given in Figure 3. Yield stresses of 42. ksi for the A36 steel and 56. ksi for the Grade 50 steel approximate the test coupon's values of the Lehigh specimens.

For the weldment elements, the results of the research of Butler and Kulak (4) are used. The force-deformation curve for fillet welds in shear is shown in Figure 4. This curve is for a 1/4" E60 weld one-inch in length. To obtain the strength and stiffness of the welds of different weld sizes, grades, and tributary lengths, the procedure given in Eighth Edition of the AISC Manual (see pp. 4-73) was used. The Richard Equation (4) was used to analytically represent force-deformation curves and is plotted in Figure 4. For the 1/4" E60 weld, this equation is

$$R = \frac{5000 \times \Delta}{\left(1 + \left|\frac{5000. \times \Delta}{11.}\right|\right)}$$

where R is the load and Δ is the deformation.

For the butt welds of Specimen 2, the strength and stiffness of these welds were taken equal to the doubler plate strength and stiffness.

IV. Analytical Results.

Shown in Figure 5 is a typical computer plot of the undeformed and deformed shape of the test specimens as obtained from the finite element analysis. The deformed shape is exaggerated to show the distortion pattern of the specimens. It is of interest to note the general distorted shape of the panel zone and also the kinking of the column flanges near the corners of the panel. Both these features were observed and reported by Krawinkler, Popov, and Bertero in their experimental studies at the University of California at Berkeley (6, 7). This plot was generated from the model of Specimen 3 and as a result the small distortion of the weldment elements may also be observed.

Figures 6, 7, 8, and 9 show the shear stress distribution along the vertical centerline of the panel as a function of the applied load. At low loads the maximum shear stress occurs at the center of the panel, whereas near maximum load the shear stress is uniform across the panel. It is noted that the shear stress in the doubler lags the shear stress intensity in the column web until near maximum load is reached. This is a direct result of the weldment distortions. Shown in Figure 10 is the panel zone deformation of Specimen 3 for a beam load of 110. kips. The <u>average</u> shear strain is approximately 0.046 radians and is computed as follows:

$$\gamma = \frac{2 \times 0.56''}{24''} = 0.046$$

This value compares almost exactly with the value obtained by averaging all of the panel zone element strains of the model.

The resultant loads and their directions on the weldment elements for Specimen 3 (fillet welded Grade 50 doubler) are shown in Figures 11 through 15 where these figures are for 20%, 40%, 60%, 80%, and 100%, respectively, for 102. kip beam loads. To compute the load per inch of weld, the load values shown in these figures must be divided by their tributary areas. For example, in Figure 15 the weldments at the corner have a load of 120.29 kips and have a total tributary length of 6.86 inches. The strength of these weldments is then computed as follows:

a) For a 1/4" weld one-inch long in shear R - 11.0 kips (see Figure 4).

b) Multiply 11.0 kips by the ratio of 70/60 to account for E70 electrodes.

c) Multiply the result above by the ratio of 3/2 to account for the 3/8" weld.

d) Multiply the result of (c) by 6.86 to account for this tributary length.

That is, the corner weldments have a strength of

$$R = 11.0 \times \frac{70}{60} \times \frac{3}{2} \times 6.86 = 132.\ \text{kips}$$

The deformation of these welds as determined from Program INELAS was 0.05 inches which is about one-half the total ductility available as reported by Butler and Kulak for welds in pure shear (see Figure 4). These results support the use of the fillet weld for doubler plates in place of the more expensive full penetration welds.

In Figure 16 the experimental load-panel zone deformation curves are shown as solid lines. The dashed lines are the results obtained by Program INELAS. The agreement between these is very good especially in the Specimens 2, 3, and 4, which have the panel zone reinforced with doubler plates. The analytical study showed that the fillet-welded specimen performed essentially identical to the butt-welded specimen.

From these results it is apparent that the panel zone itself is constrained significantly by the column flanges and the beam web so that this zone will carry a significantly greater shear load than predicted by the AISC plastic design formula

$$V_y = 0.55 F_y d_c t$$

where

v_y = shear force causing yielding in the panel zone

F_y = yield stress of steel in tension

d_c = depth of column

t = thickness of web

This fact was observed and reported by Krawinkler, Berterro, and Popov (6). Krawinkler (7) presents a panel ultimate shear strength formula based upon a panel strain of four times the yield strain. This is Equation 10 on page 87 of this reference. If the panel strain is left arbitrary, this formula becomes

$$V_u = 0.55\ F_y d_c t\ \left(1. + \frac{1.15\ b_c\ t_{cf}^2}{d_b d_c t} (\beta - 1)\right)$$

where β is the ratio of the panel strain to the yield strain. For Lehigh tests this reduces to

$$V_u = V_y\ (1. + 0.0575\ (\beta - 1))$$

A comparison of the Lehigh test results and this formula is given in the table below:

SPECIMEN	LEHIGH TEST LOAD	TEST PANEL SHEAR	FORMULA
#1 @ $\gamma = 1.75\%$	$55.^k$	210.6^k	$201.^k$
#2 @ $\gamma = 2\%$ (1st Cycle)	$100.^k$	$383.^k$	$454.^k$
#2 @ $\gamma = 2\%$ (7th Cycle)	$110.^k$	$421.^k$	$454.^k$
#4 @ $\gamma = 2\%$ (1st Cycle)	$90.^k$	$344.^k$	$455.^k$
#4 @ $\gamma = 2\%$ (7th Cycle)	$100.^k$	$383.^k$	$455.^k$

Krawinkler specifically states that his derivation should be valid for $(\beta - 1)$ values (his γ/γ_y values) up to 3; however, the agreement is fair for the Lehigh tests even for $(\beta - 1)$ values of the order of 7. He also indicates that the formula is in good argrement with experimental results for joints with thin to medium-thick column flanges, but that for very thick flanges (greater than two inches), additional studies are required. It should be noted that very significant increases in allowable panel shears result when this method is used as is evident in his design aid given in Figure 8 of his paper. These increases range from about 10% up to about

65% for the W14 sections shown. It is apparent from the proposed shear strength equation that the increase in shear capacity is primary a function of the panel zone aspect ratio and the column flange thicknesses.

Krawinkler further recommends that the effect of the normal stresses in the panel zone due to the column axial load be accounted for by the factor, α, where

$$\alpha = \sqrt{1 - \left(\frac{P}{P_y}\right)^2}$$

This is his Equation 5 in which P is the axial column load and P_y is the yield axial load.

Two additional studies were made using the finite element models for Specimens 1 and 2. These were (a) the flange continuity plates were removed from the models and (b) the beam tip loads were removed and their effects were introduced as concentrated flange forces at the column faces and a concentrated shear in the beam web at the column faces. The panel zone strain distribution obtained from these models did not vary significantly from those obtained previously. Further study concerning the removal of the flange continuity plates, however, should be made in the full scale tests since the analytical model is a two-dimensional model and does not account for out-of-plane bending of the beam flanges.

V. Summary and Conclusions.

This analytical study of the Lehigh test specimens indicates that the finite element Program INELAS adequately predicts the first half cycle behavior of the test specimens and provides valuable insight into the load and strain distribution within the panel zone. These results are in agreement with and support the analytical and experimental work at the

University of California at Berkeley. This latter observation is significant in that the California researchers have developed a panel shear strength formula which includes the beneficial effects of the boundary elements of the panel zone; i.e., the column flanges and the beam web. This formula, with an allowable prescribed panel zone shear strain, makes it possible for the structural designer to arrive at a panel shear strength in a rational way.

REFERENCES

1. "Tests of Panel Zone Behavior in Beam-Column Connections" by Roger G. Slutter, Report No. 200.81.403.1, Fritz Engineering Laboratory, Lehigh University.

2. "User's Manual for Nonlinear Finite Element Analysis Program INELAS", by Ralph M. Richard, Department of Civil Engineering, The University of Arizona, Tucson, Az, 1968.

3. "Finite Element Analysis of Inelastic Structures", by Ralph M. Richard and James R. Blacklock, AIAA Journal, Vol. 7, No. 3, March 1969.

4. "Strength of Fillet Welds as a Function of Direction of Load", by L. J. Butler and G. L. Kulak, Welding Journal Research Supplement, May 1971.

5. "A Versatile Elastic-Plastic Stress-Strain Formula", by Ralph M. Richard, Journal of the Engineering Mechanics Division, ASCE, August 1975.

6. "Shear Behavior of Steel Frame Joints", by H. Krawinkler, V. V. Bertero, and E. P. Popov, Journal of the Structural Division, ASCE, November 1975.

7. "Shear in Beam-Column Joints in Seismic Design of Steel Frames", by H. Krawinkler, Engineering Journal, AISC, Third Quarter 1978.

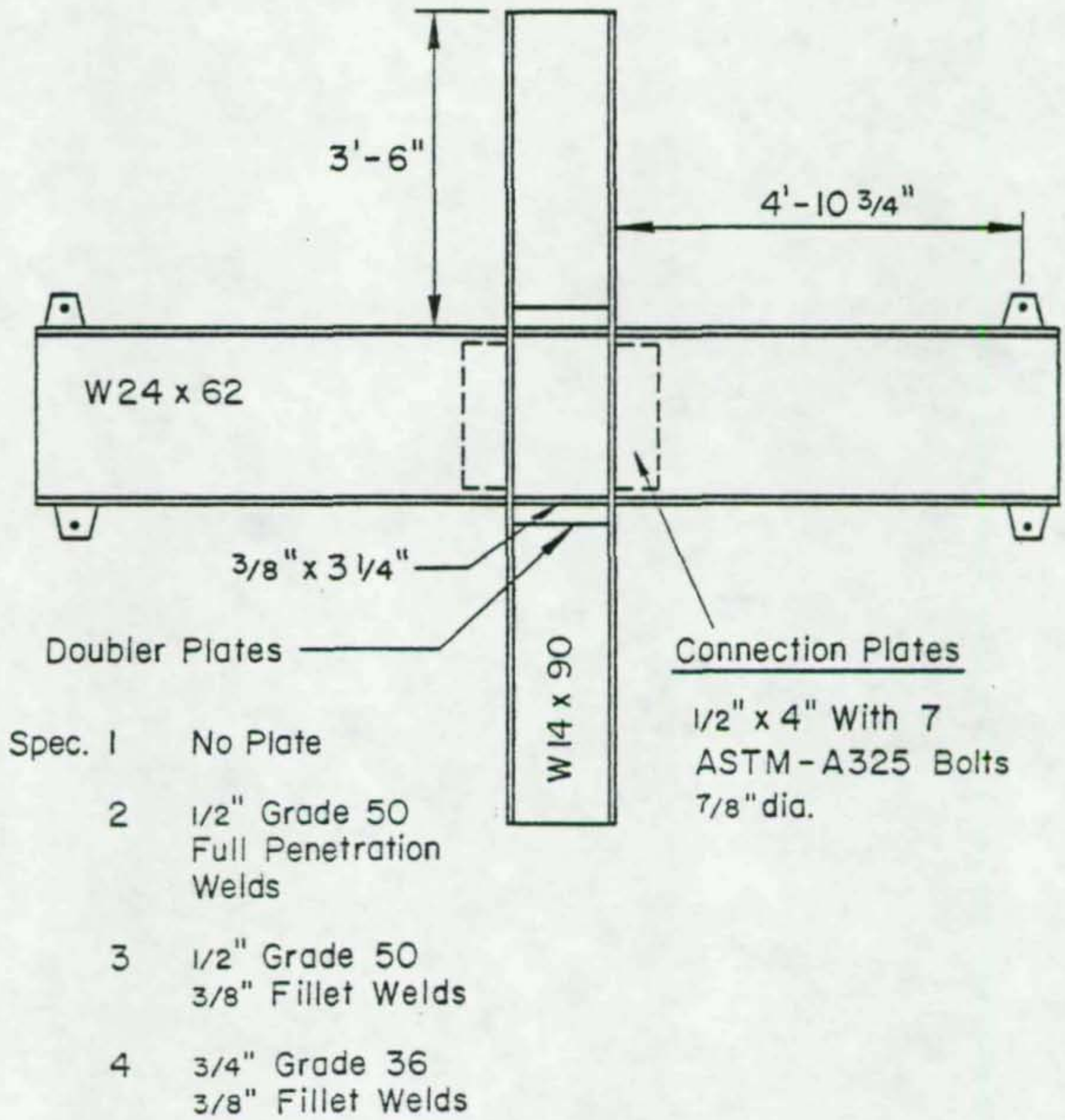

Fig. 1 Dimensions of Test Specimens

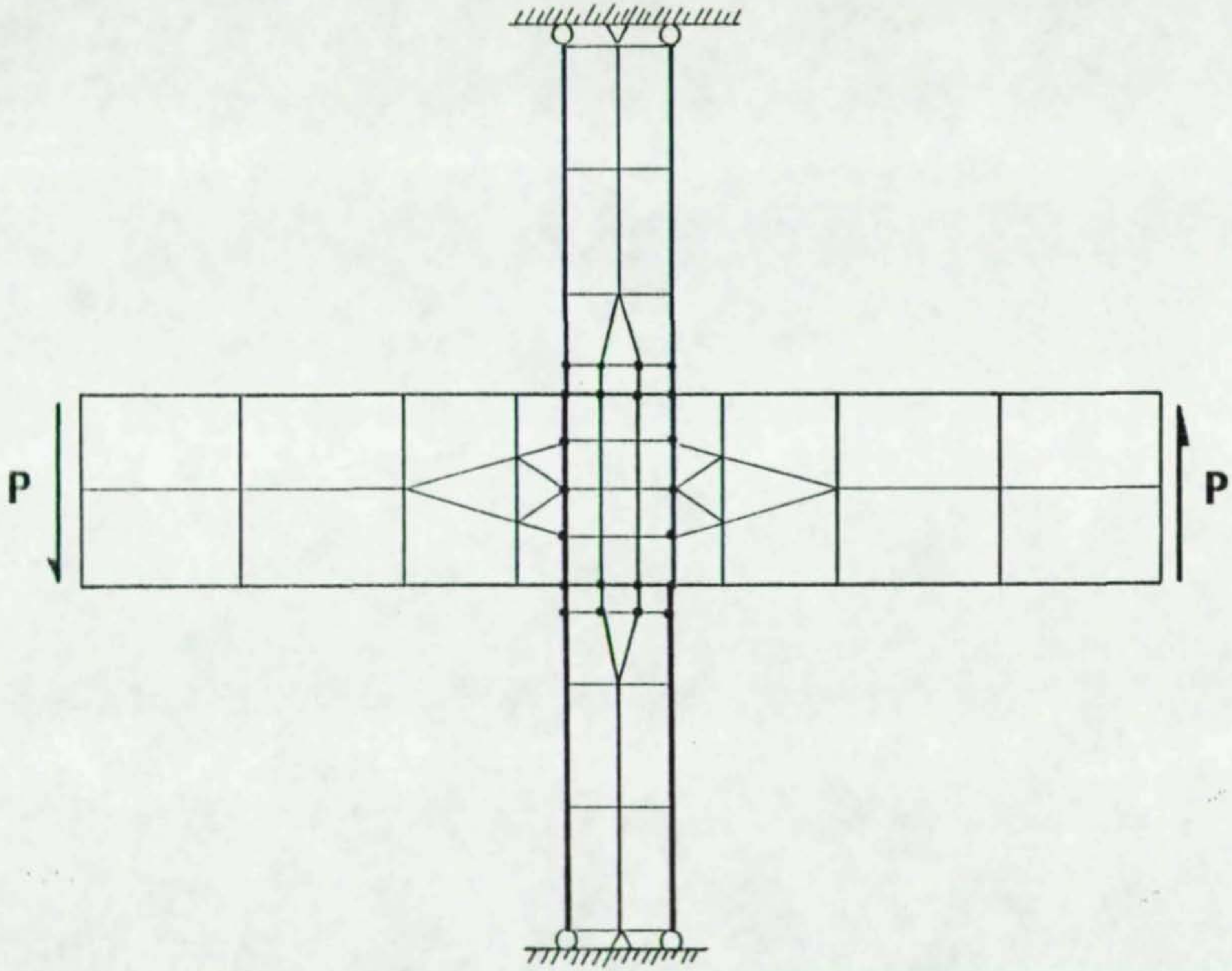

Fig. 2 Test Specimen Model with Weld Elements

A-36

$$\sigma = \frac{30\times10^{3}\times\varepsilon}{\left(1+\left|\frac{30\times10^{3}\varepsilon}{56.}\right|^{8}\right)^{1/8}}$$

Grade 50

$$\sigma = \frac{30\times10^{3}\times\varepsilon}{\left(1+\left|\frac{30\times10^{3}\varepsilon}{56.}\right|^{5}\right)^{1/5}}$$

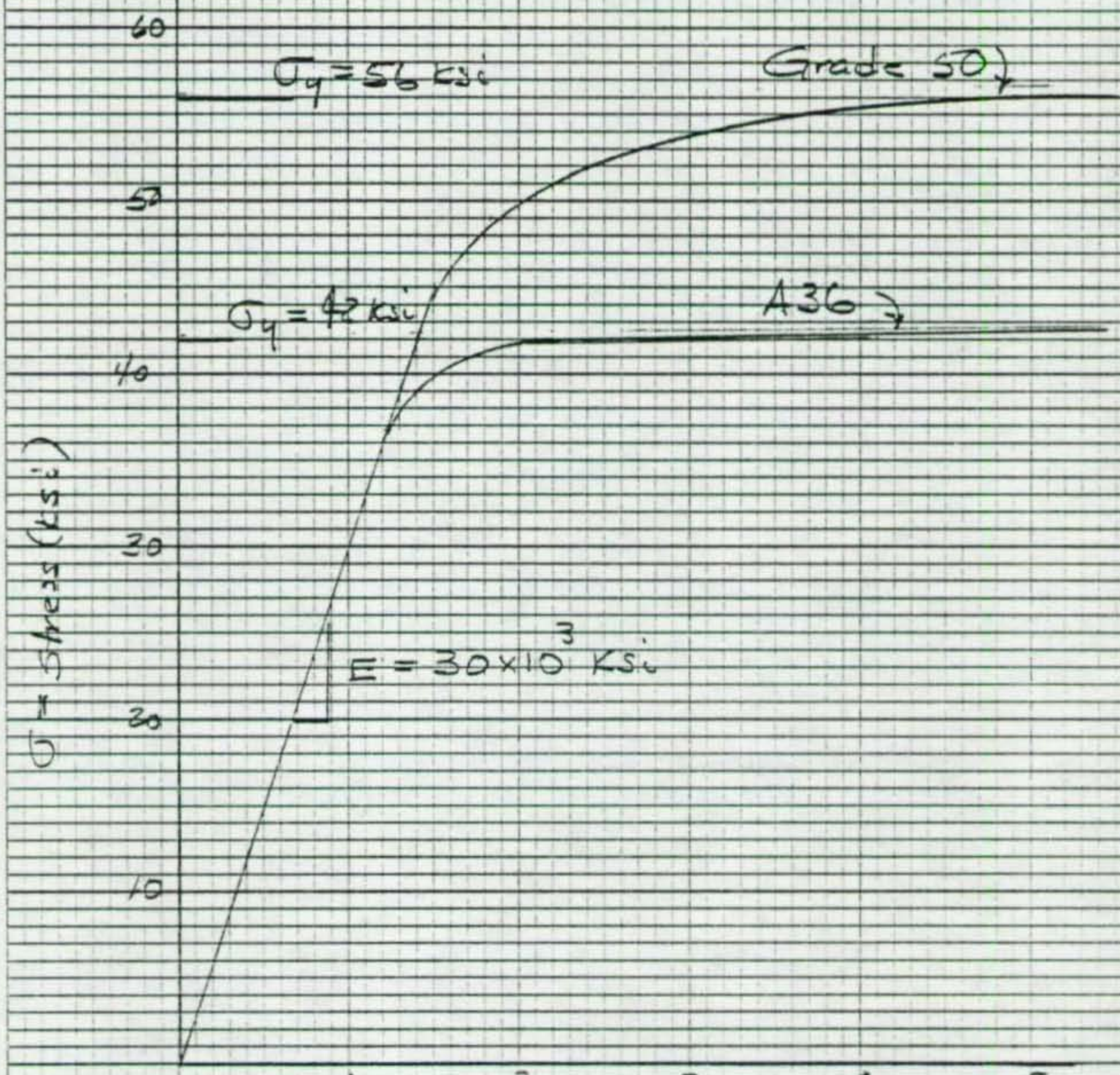

Figure 3. Steel Stress-Strain Curves

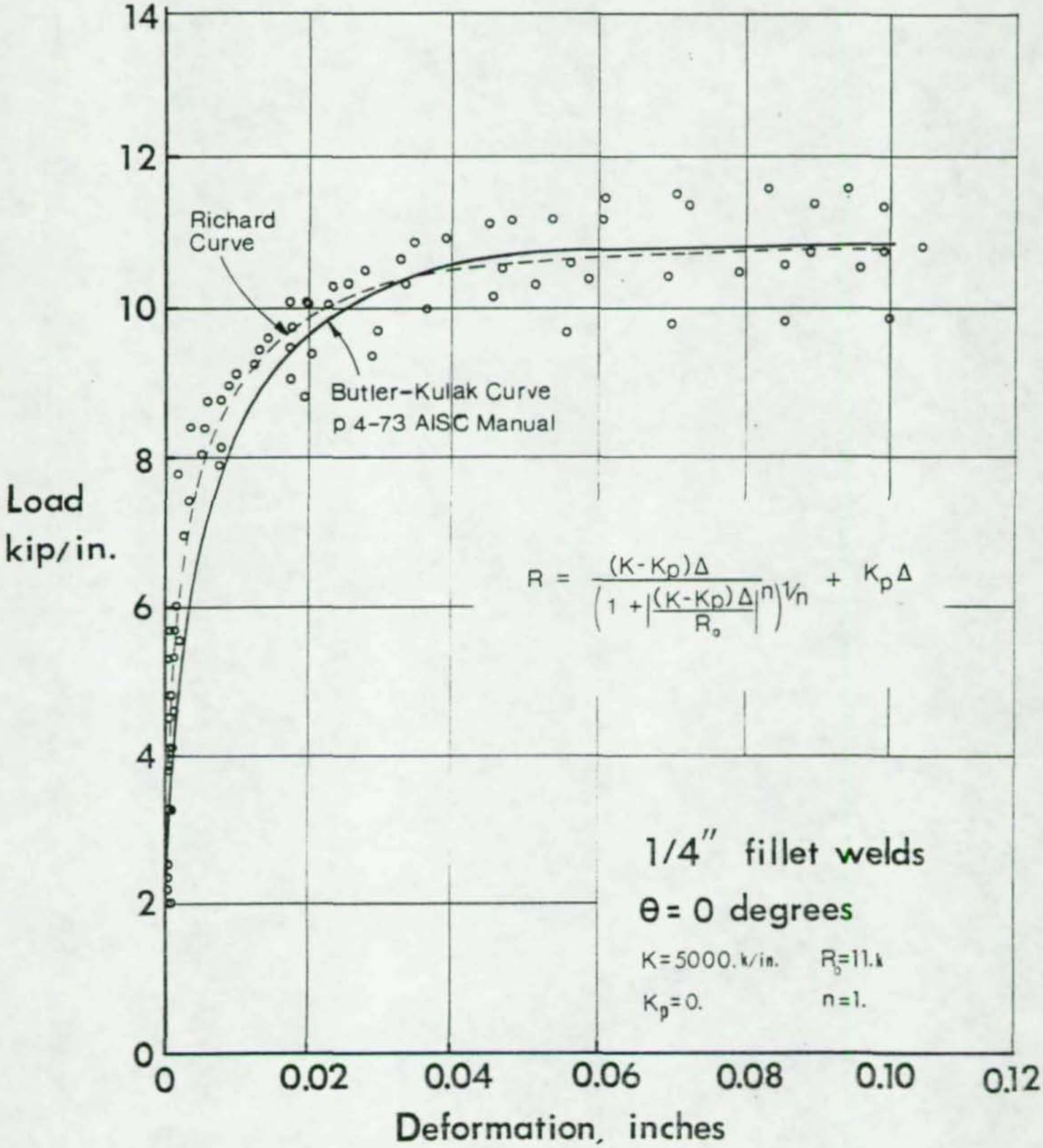

Richard Curve
Butler-Kulak Curve
p 4-73 AISC Manual
Load kip/in.
$R = \dfrac{(K-K_p)\Delta}{\left(1+\left|\dfrac{(K-K_p)\Delta}{R_o}\right|^n\right)^{1/n}} + K_p\Delta$
1/4" fillet welds
θ = 0 degrees
K = 5000. k/in.
R_o = 11. k
K_p = 0.
n = 1.
0
2
4
6
8
10
12
14
0
0.02
0.04
0.06
0.08
0.10
0.12
Deformation, inches

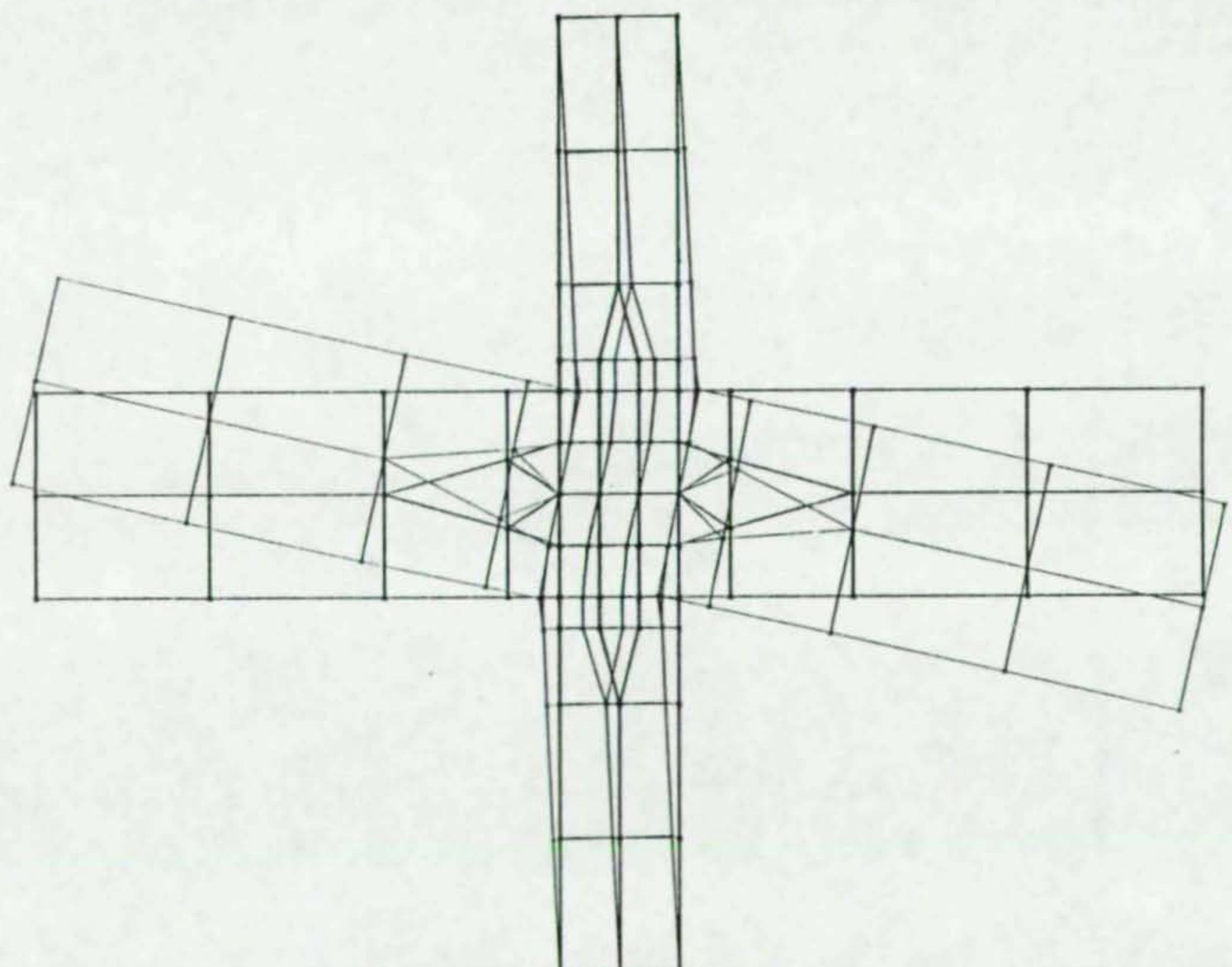

Fig. 5 DOUBLER PLATE

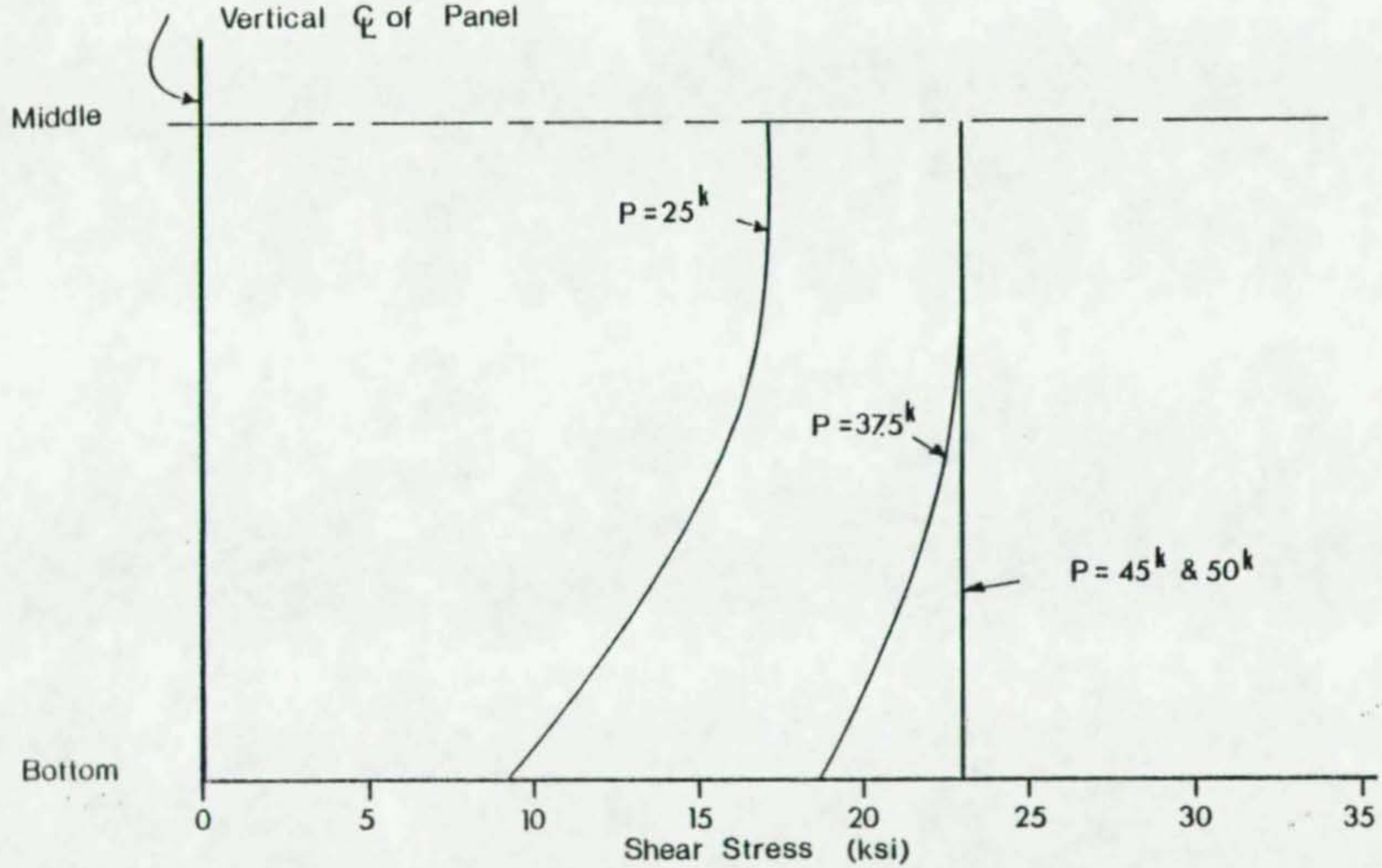

Fig. 6 Panel Zone Shear Stress

(Specimen 1)

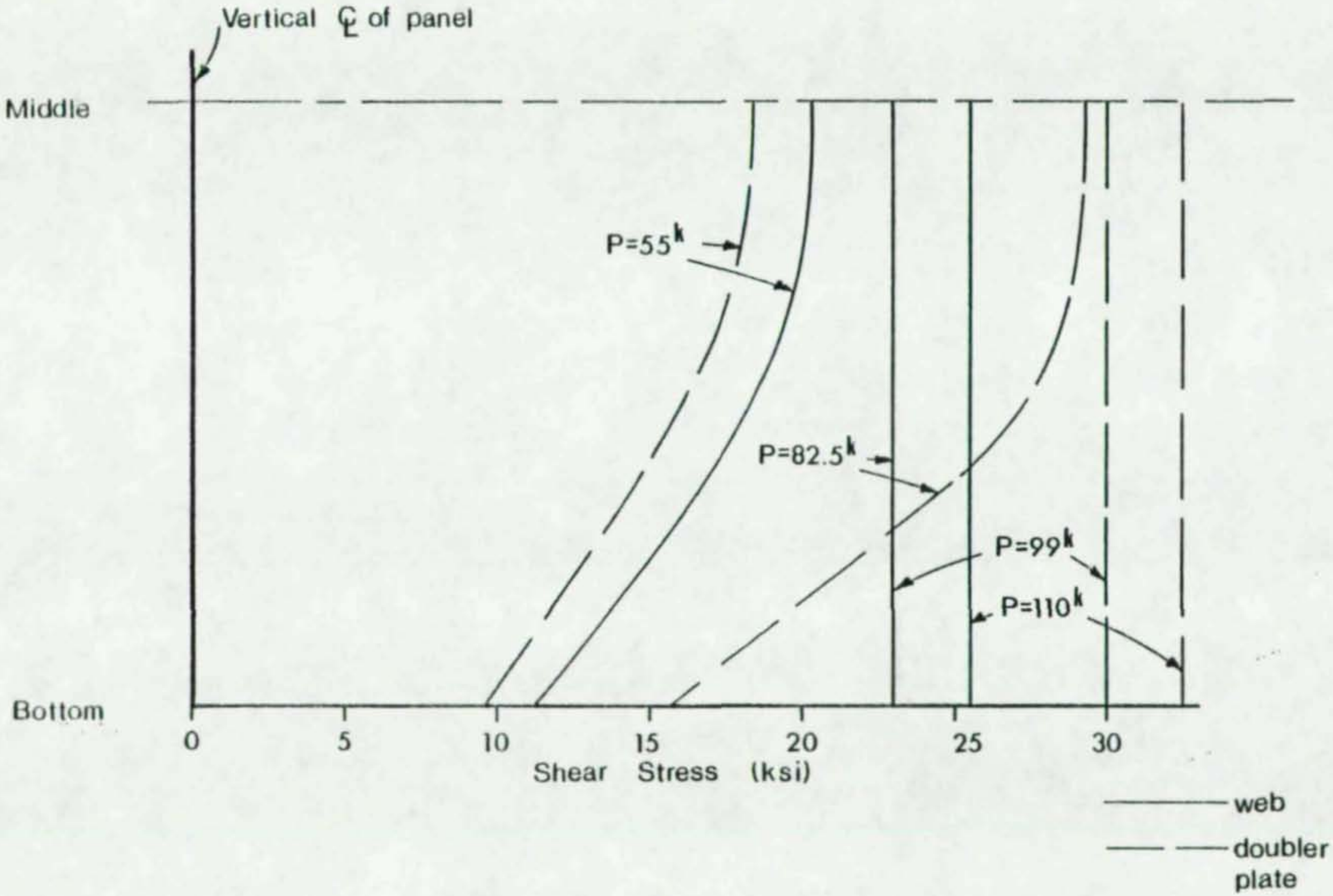

Fig. 7 Panel Zone Shear Stress (Specimen 2)

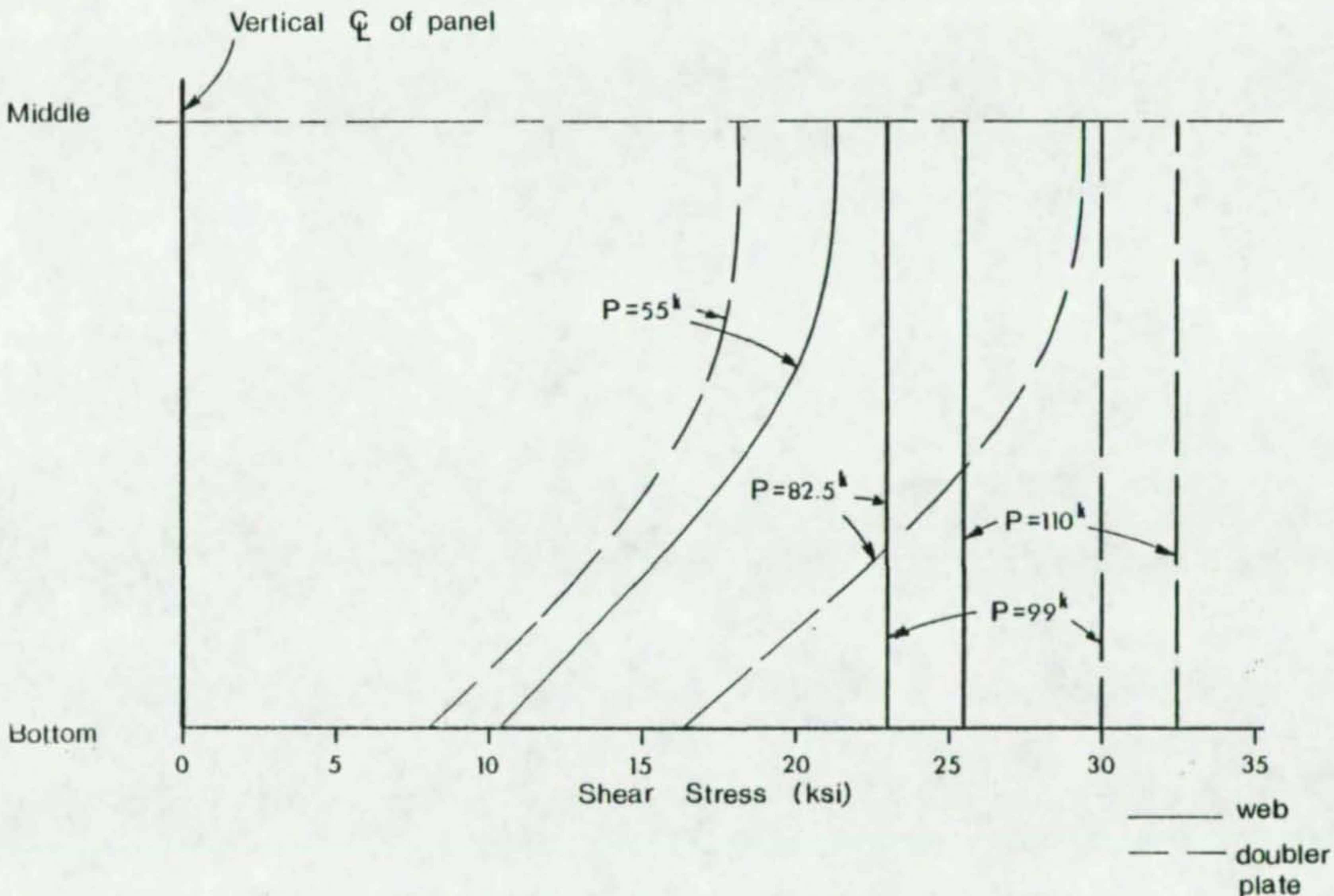

Fig. 8 Panel Zone Shear Stress (Specimen 3)

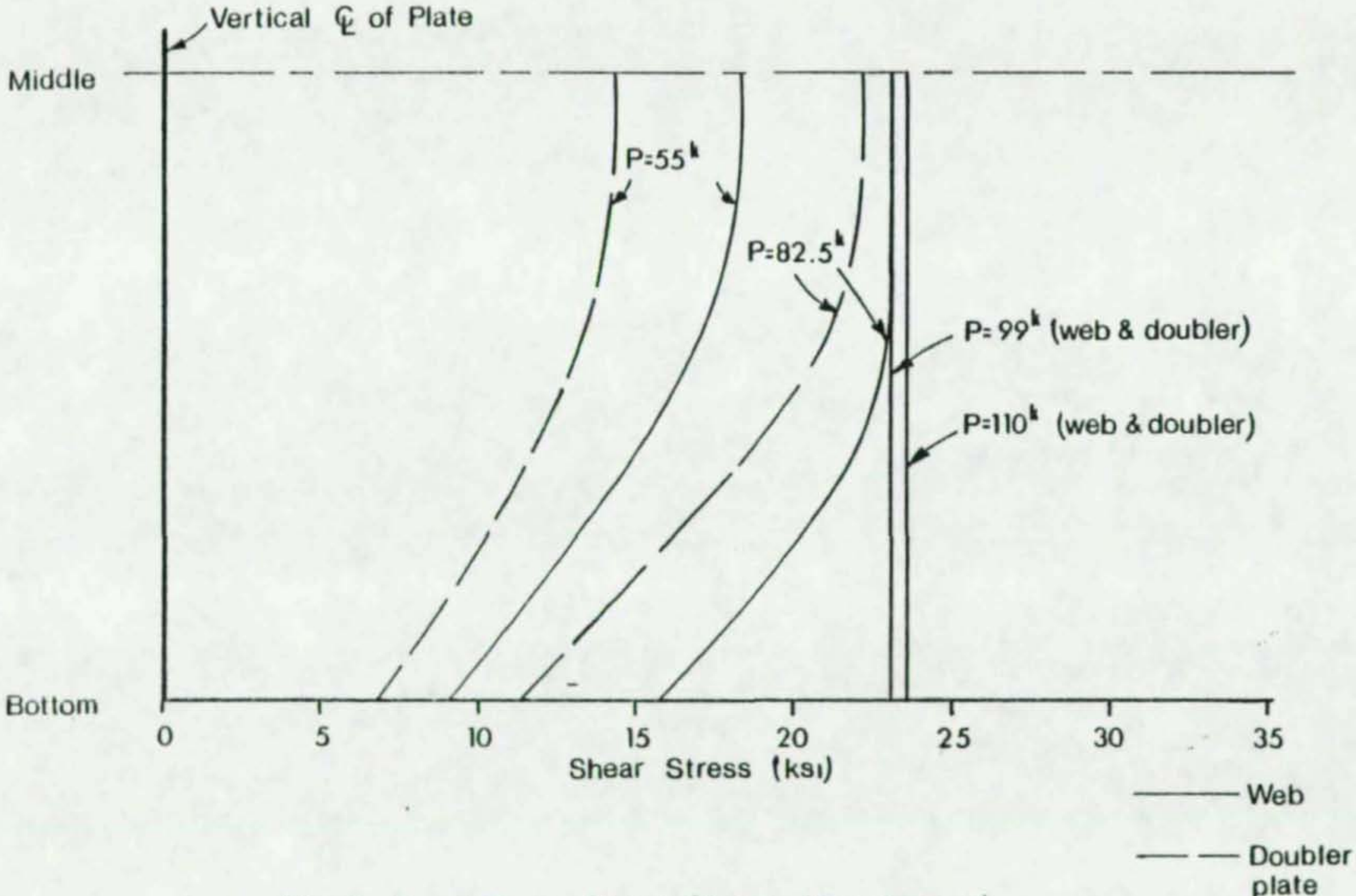

Fig. 9 Panel Zone Shear Stress (Specimen 4)

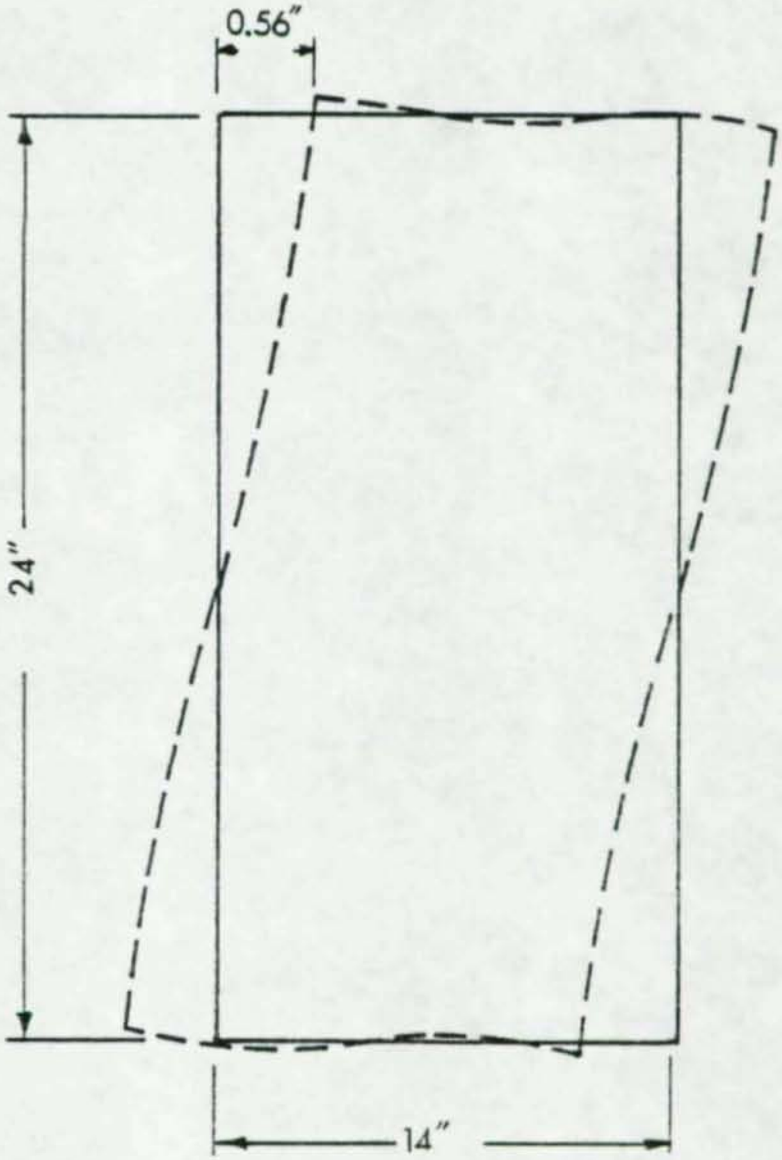

Fig. 10 Pane Zone Deformation for Specimen 3 at $P = 110^{k}$

Shear Strain: $\gamma = 0.046$ radians

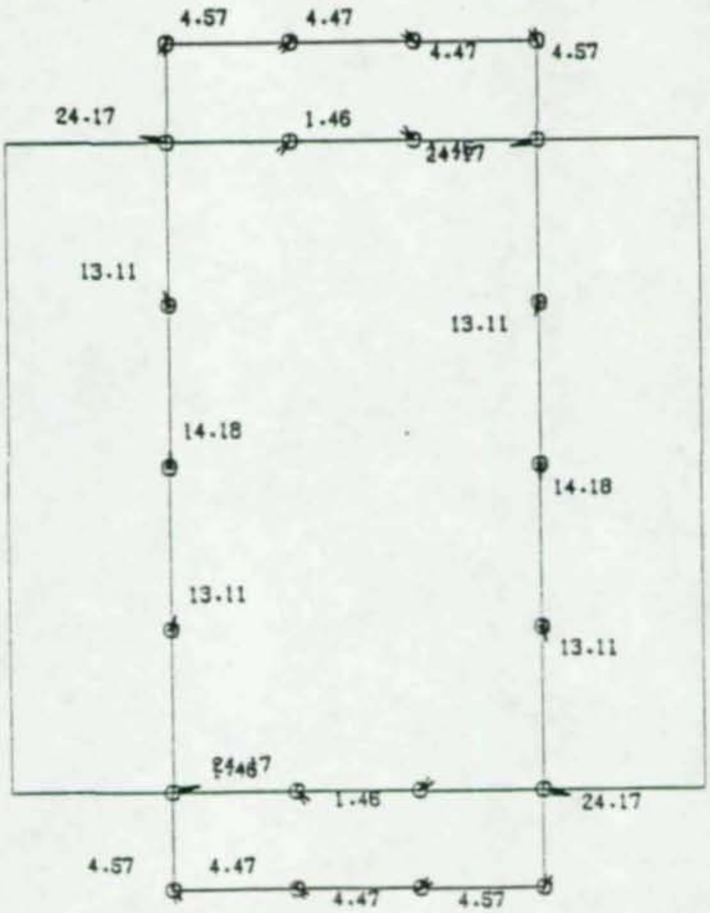

Fig. 11 LOAD 1 : RESULTANT
DOUBLER PLATE

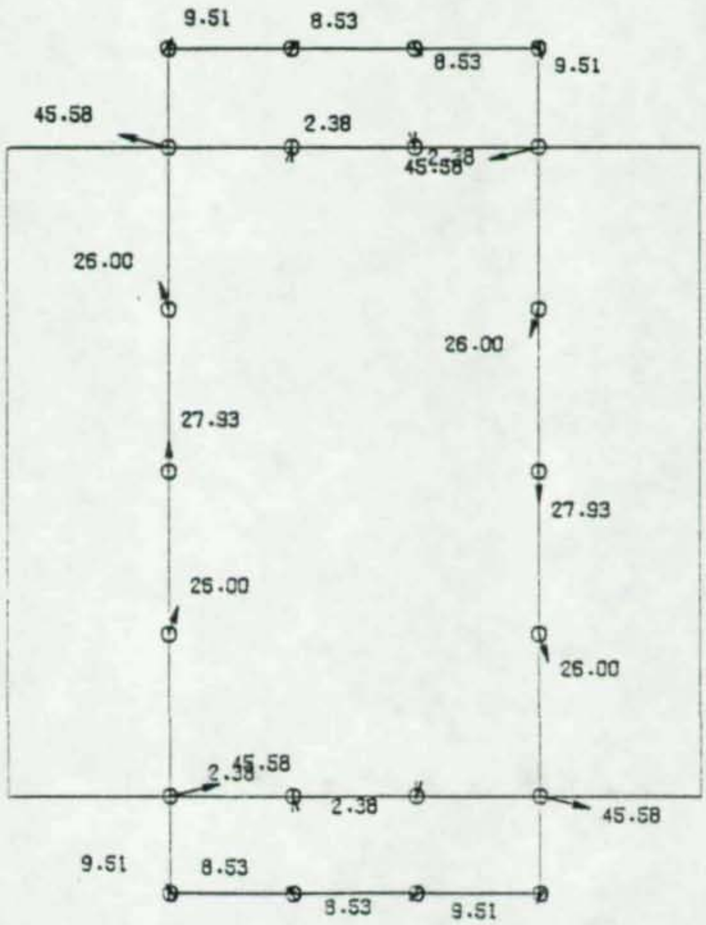

Fig. 12 LOAD 2 : RESULTANT
DOUBLER PLATE

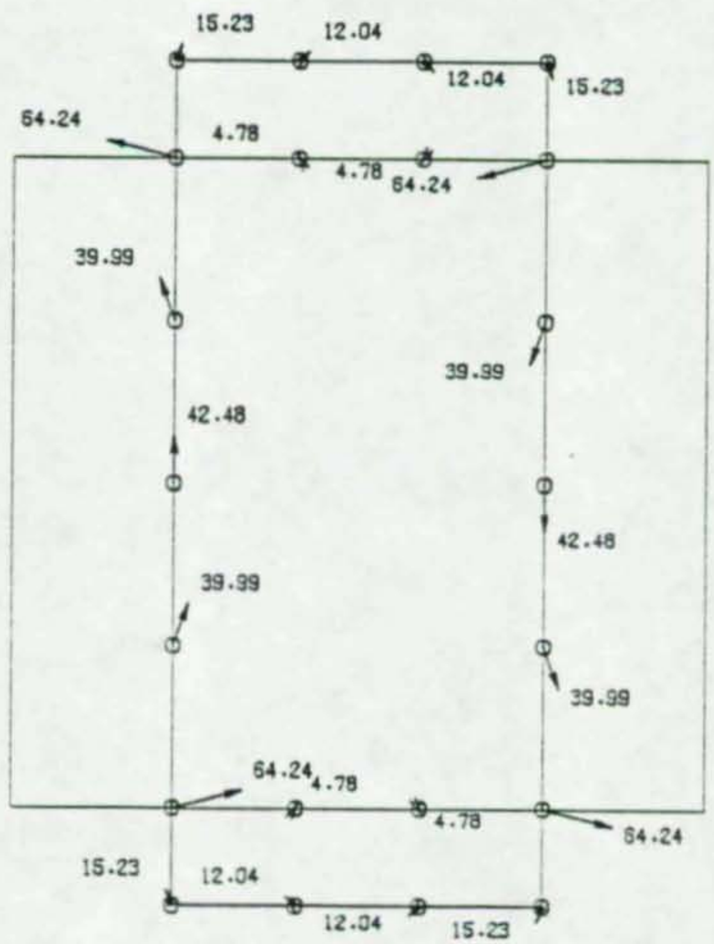

Fig. 13 LOAD 3 : RESULTANT
DOUBLER PLATE

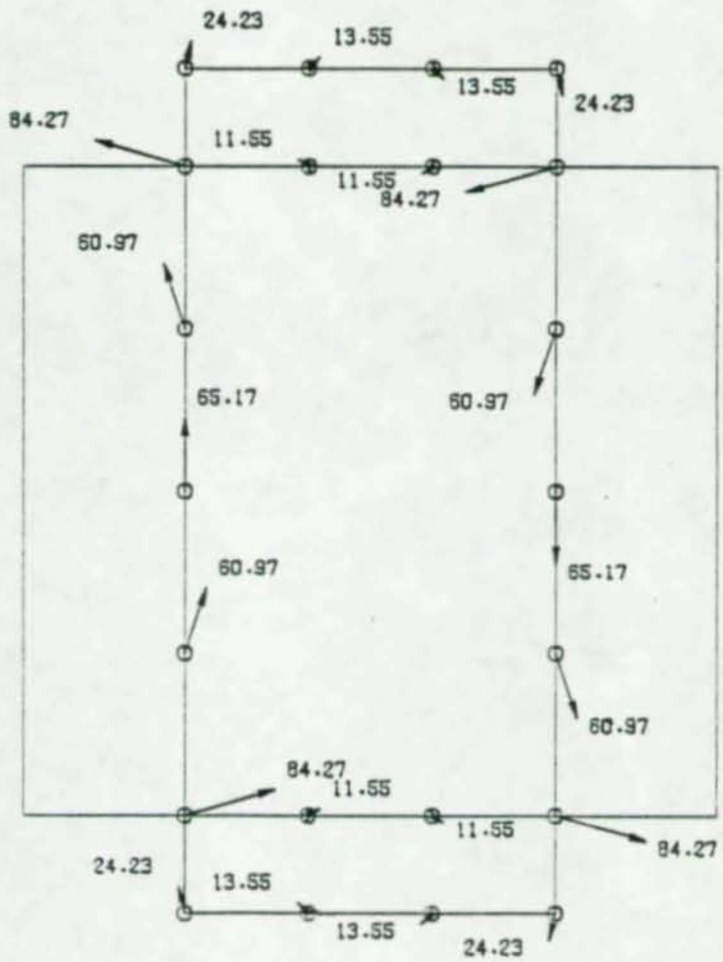

Fig. 14 LOAD 4 : RESULTANT
DOUBLER PLATE

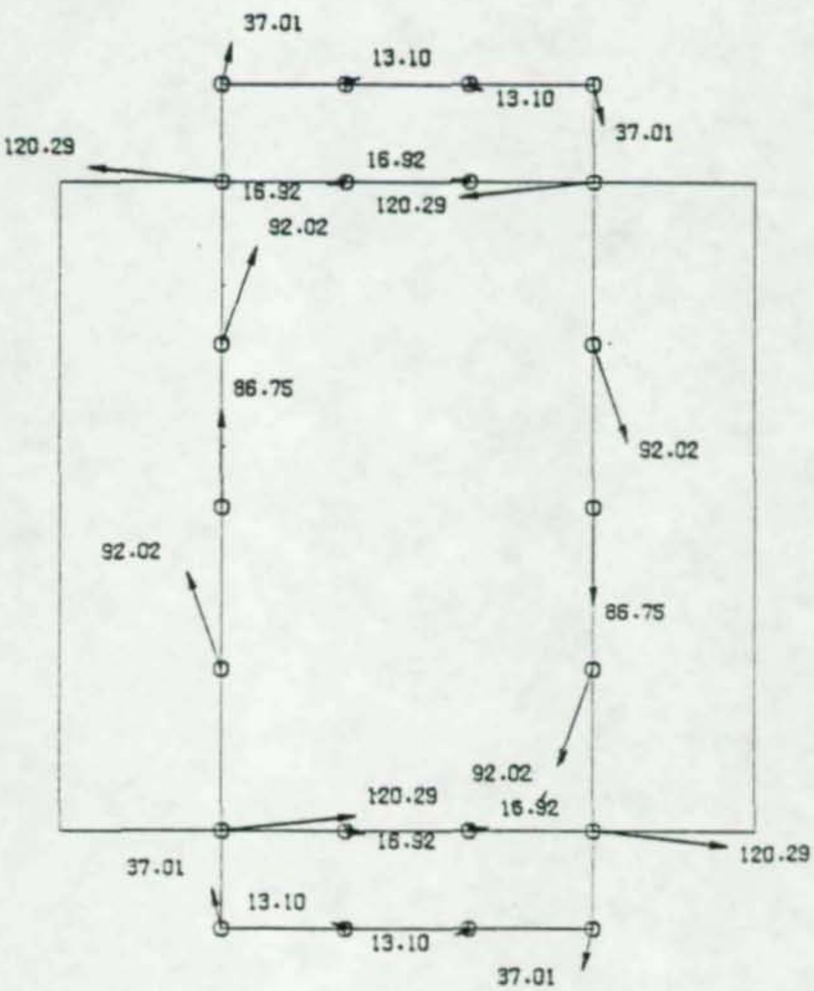

Fig. 15 LOAD 5 : RESULTANT DOUBLER PLATE

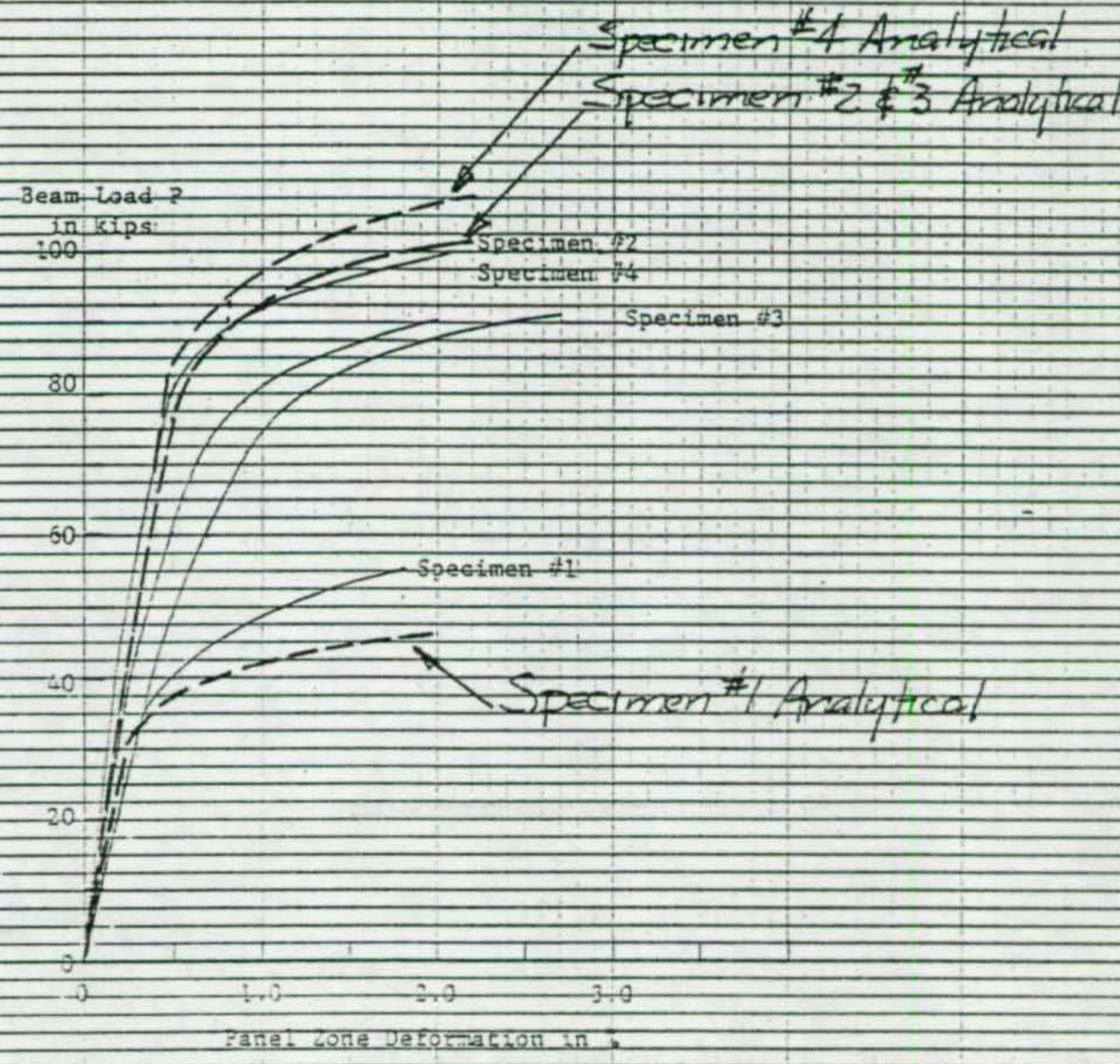

Fig. 16 Load versus Panel Zone Deformation for First Half Cycle of Loading